Uniaxial pressure effects on spin-lattice coupled phase transitions in a geometrical frustrated magnet $CuFeO_2$

H. Tamatsukuri,* S. Aoki, S. Mitsuda, T. Nakajima,† T. Nakamura, T. Itabashi, S. Hosaka, and S. Ito
Department of Physics, Faculty of Science, Tokyo University of Science, Tokyo 162-8601, Japan

Y. Yamasaki† and H. Nakao
High Energy Accelerator Research Organization, Tsukuba, Ibaraki 305-0801, Japan

K. Prokes and K. Kiefer
Helmholtz-Centre Berlin for Materials and Energy, Hahn-Meitner-Platz 1, Berlin 14109, Germany
(Received 8 June 2016; revised manuscript received 7 September 2016; published 1 November 2016)

We performed magnetic susceptibility, dielectric constant, neutron-diffraction, and synchrotron radiation x-ray diffraction measurements on a spin-lattice coupling system $CuFeO_2$ under applied uniaxial pressure p up to 600 MPa. We found that the phase-transition temperature T_{N1} from the paramagnetic phase to the partially disordered phase increases by as much as 5 K from the original $T_{N1} \simeq 14$ K under applied p of 600 MPa, and that the lattice constant b_m of $CuFeO_2$ changes significantly. In contrast, the value of q_0, which is the magnetic modulation wave number at T_{N1} and which should reflect the ratios of the exchange coupling constants, is not changed, even by applied p of 600 MPa. Based on these results, we show that an explanation using only the exchange striction effect is not suitable for the magnetic phase transition in $CuFeO_2$. These results suggest that a lattice degree of freedom via a spin-lattice coupling is indispensable for the determination of the magnetic properties of $CuFeO_2$. A dielectric anomaly under applied p of 600 MPa is also briefly discussed.

DOI: 10.1103/PhysRevB.94.174402

I. INTRODUCTION

Geometrically frustrated magnets provide fertile fields for modern condensed-matter physics research [1]. In order to lift the large degeneracy of their ground states resulting from the frustration, the systems tend to closely connect lattice degrees of freedom with spins. As a result, the spin-lattice couplings in the geometrically frustrated magnets give rise to exotic magnetic phenomena, such as spin-Peierls transition [2,3], spin-driven Jahn-Teller effect [4,5], and spin-driven ferroelectrics [6].

Among the spin-lattice coupled systems, the delafossite compound $CuFeO_2$ (CFO) is one material that has been extensively investigated in order to understand the highly rich magnetic phase diagram including the spin-driven ferroelectric phase [7–20]. CFO belongs to the $R\bar{3}m$ space group at room temperature ($a = b = 3.03$ Å, $c = 17.17$ Å in hexagonal notation). In CFO, Fe^{3+} ions ($S = 5/2$) form triangular-lattice layers with antiferromagnetic interactions, which are stacked along the c axis. As shown in Fig. 1, with decreasing temperature (T) from a paramagnetic (PM) phase, the system enters a partially disordered (PD) phase with a magnetic modulation wave vector $(q,q,3/2)$ [$q = 0.196$–0.220] at $T_{N1} = 14$ K, in which the amplitude of spins along the c axis is sinusoidally modulated [21,22]. On further cooling to $T_{N2} = 11$ K, a collinear 4-sublattice (4SL) phase ($\uparrow\uparrow\downarrow\downarrow$) with a magnetic modulation wave vector $(1/4,1/4,3/2)$ is realized [21,23].

These magnetic phase transitions are accompanied by a spontaneous lattice distortion from rhombohedral $R\bar{3}m$ to monoclinic $C2/m$ [9,11]. In the lattice distortion, the monoclinic b axis (b_m) elongates and the monoclinic a axis (a_m) contracts, resulting in a deformation from the equilateral triangular lattice in the PM phase to a scalene one in the 4SL phase, through an isosceles triangular lattice in the PD phase [10,19], as shown in Fig. 1. Hereafter, we add the subscript "m" to the monoclinic notations, and the [110] and the $[1\bar{1}0]$ directions in hexagonal notation correspond to $[010]_m$ and $[100]_m$ directions in monoclinic notation, respectively (see Fig. 1). Several researchers have pointed out that the spin-lattice coupling in CFO systems plays a key role in the realization of the collinear $\uparrow\uparrow\downarrow\downarrow$ magnetic structure as the ground state [9,10], which is originally not expected from the Heisenberg spin character of Fe^{3+} ion. This point is also consistent with theoretical work that the spin-lattice coupling stabilizes the collinear magnetic structures including the 4SL $\uparrow\uparrow\downarrow\downarrow$ structure, even in Heisenberg antiferromagnets [24]. Moreover, the nearest-neighbor exchange interaction J_1 splits into three inequivalent interactions due to the the monoclinic lattice distortion. The split interactions successfully account for spin-wave excitation in the 4SL phase [25] and electron spin resonance (ESR) spectrum [26].

In addition to the investigations into the origin of the ground state and the value of the exchange constants at low temperature, the effects of pressure on the magnetic properties of CFO have also been investigated [16–19]. Because the lattice symmetry is broken by the spontaneous lattice distortion just at the magnetic phase transition temperature T_{N1}, one expects that the application of pressure at this temperature has a significant influence on the magnetic properties of CFO. Therefore, we focus on the effects of pressure on the exchange

*tamatsukuri@nsmsmac4.ph.kagu.tus.ac.jp
†Present address: RIKEN Center for Emergent Matter Science (CEMS), Saitama 351-0198, Japan.

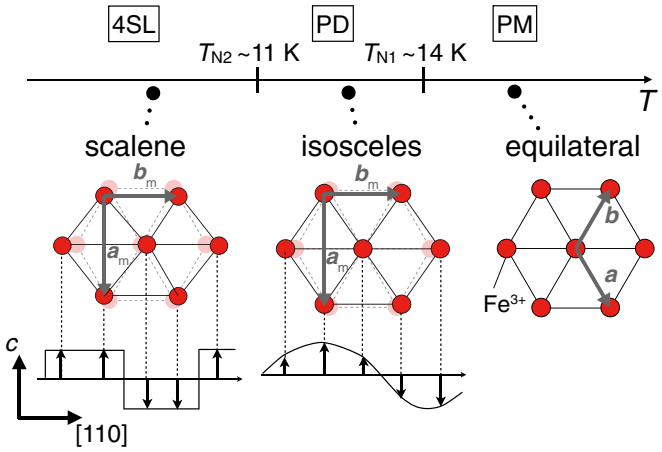

FIG. 1. Magnetic phase diagram of CFO as a function of temperature. Below $T_{N2} \simeq 11$ K, a collinear 4-sublattice (4SL) phase ($\uparrow\uparrow\downarrow\downarrow$) with a magnetic modulation wave vector (1/4,1/4,3/2) is realized. In the range $T_{N2} \leqslant T \leqslant T_{N1} \simeq 14$ K, a sinusoidal magnetic structure with a magnetic modulation wave vector $(q,q,3/2)$ [$q = 0.196$–0.220] is realized. Triangular lattices formed by Fe^{3+} ions in each phase are also schematically illustrated.

constants at T_{N1}. Although, in the vicinity of T_{N1}, it is rather difficult to determine the exchange constants from spin waves, a magnetic modulation wave number "at T_{N1}", q_0, can be determined by the ratio of exchange constants in general, and thus it should be a characteristic value.

Using neutron diffraction under an "isotropic" pressure up to 8 GPa, which suppresses the spontaneous lattice distortion, Terada *et al.* reported that q_0 is varied from 0.195 (0 Pa) to ~0.185 (5 GPa) by the isotropic pressure, together with the rise of T_{N1} [17,27].

On the other hand, Nakajima *et al.* performed neutron-diffraction measurements under an "anisotropic" uniaxial pressure up to 100 MPa along the [1$\bar{1}$0] direction, which is the conjugate direction to the spontaneous lattice distortion in CFO [18]. Although they observed an upward shift of T_{N1}, which can be interpreted as a result of the partial release of the frustration in this system through the assistance of the spontaneous lattice distortion, a change in q_0 by the uniaxial pressure was not conclusive. Taking into account that uniaxial pressure p breaks the lattice symmetry, one can expect that a change in the ratio of the exchange constants by applied p is larger than those by the isotropic pressure, and that q_0, which should reflect the ratio of the exchange constants, also shows larger change. Nevertheless, applied p up to 100 MPa is too small to allow the investigation of the p variation of q_0.

Quite recently, we developed a technique that enables the application of the uniaxial pressure p up to 600 MPa for CFO. In this paper, we report the results of magnetic susceptibility, dielectric constant, neutron-diffraction, and synchrotron radiation x-ray diffraction measurements on CFO under applied p up to 600 MPa. We found that the value of q_0 is not changed even by applied p of 600 MPa despite a drastic increase in T_{N1}. Moreover, the applied p of 600 MPa causes remarkable change in the b_m beyond the spontaneous lattice distortion. Taking into account the exchange striction effect that the exchange constants determining q_0 are varied by the change in the lattice constants, these results provide a strict condition for the p variation of the exchange constants. Based on the mean-field approximation within this condition, we calculated an enhancement factor of T_{N1}. As a result, we found that the observed enhancement of T_{N1} is not explained by the exchange striction effect. Our study suggests that the lattice degree of freedom in a spin Hamiltonian via the spin-lattice coupling is indispensable for the determination of magnetic properties of CFO.

II. EXPERIMENTAL DETAILS

A single crystal of CFO was prepared by the floating-zone method [28]. The crystal was cut into a dicelike shape with typical dimensions of $1.36 \times 1.44 \times 1.70$ mm^3. The three axes of the dicelike sample are along the [110], [1$\bar{1}$0], and [001] directions, and the sample was mounted in a pressure cell used in Refs. [18,19,29] with the [1$\bar{1}$0] axis vertical. By adopting the dicelike shape, which is found to be more durable than the rectangular plate shape used in the previous works, we can apply the maximum force (2000 N) permitted by our uniaxial pressure devices. Moreover, by reducing the pressure surface area of the sample, finally, we have achieved the application of p up to 600 MPa, while we use the same pressure cell. The uniaxial pressure devices used in this work were the same as used in the previous studies: p along the vertical direction (therefore, $p \parallel$ [1$\bar{1}$0]) is controlled by a SiCr coil spring and a micrometer attached to the top of the cryostat, enabling us to control the magnitude of p even when the sample is at low temperatures, and p is monitored by a load meter. In all of the experiments in this study, p was always applied at 25 K. The temperature dependence of the magnetic susceptibility at the magnetic field of 100 Oe along the [1$\bar{1}$0] direction was measured by using a superconducting quantum interference device (SQUID) magnetometer (Quantum Design). The dielectric constant ϵ was measured at 10 kHz using an LCR meter (Agilent 4980A), where the electrodes consisted of silver paste painted onto [110] surfaces.

Neutron-diffraction measurements under applied p were carried out using the two-axis diffractometer E4 at the Berlin Neutron Scattering Center in the Helmholtz-Centre Berlin for Materials and Energy. The wavelength of the incident neutron was 2.44 Å. The synchrotron radiation x-ray diffraction measurements under applied p were conducted on the beam line BL-3A at the Photon Factory in High Energy Accelerator Research Organization, Tsukuba, Japan. The energy of the incident x ray was tuned to 14 keV. Since the direction of p is parallel to the [1$\bar{1}$0] direction, the scattering plane is the (H,H,L) plane in both of the diffraction measurements. Basically, we performed these diffraction measurements in the same manner as in the previous experiments [18,19].

III. RESULTS

Figure 2(a) shows the temperature dependence of magnetic susceptibility under ambient pressure and applied p of 600 MPa. At zero applied pressure, the T dependence of magnetic susceptibility is consistent with previous results [18,30]. With increasing p, T_{N1} drastically increases. The rise of T_{N1} under applied p of 600 MPa reaches 5 K from the

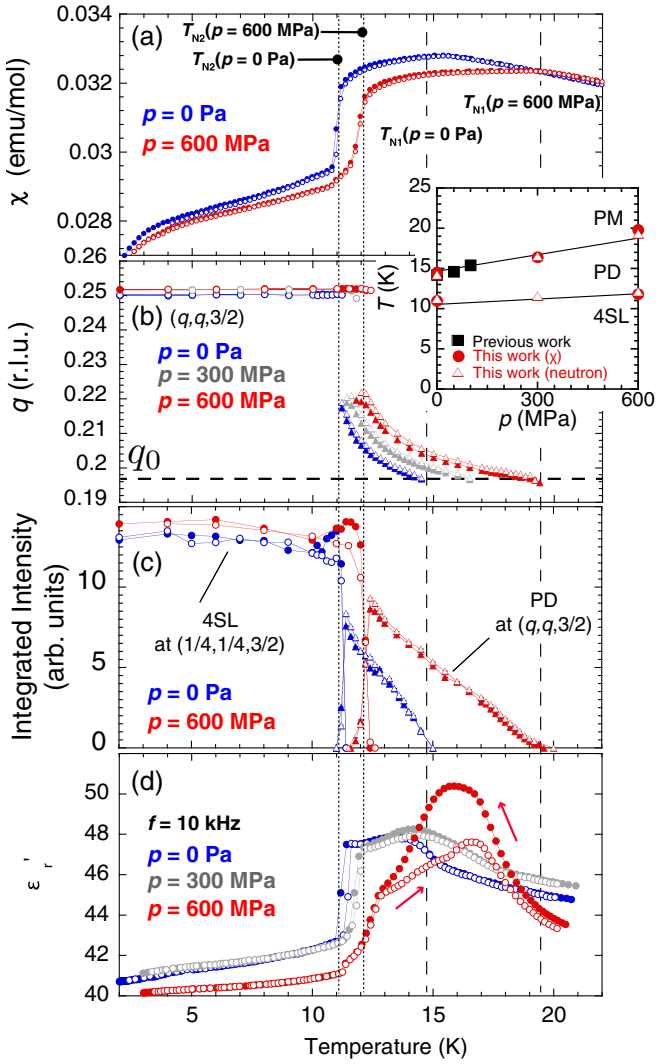

FIG. 2. Temperature dependence of (a) magnetic susceptibility χ, (b) magnetic modulation wave number q, (c) integrated intensity of the magnetic Bragg reflections, and (d) (real part of) dielectric constant ϵ along the [110] axis, of CFO under the selected applied p. Open and closed symbols denote data for increasing and decreasing temperature processes, respectively. The figure extending over (a) and (b) shows a p-T phase diagram of CFO. The data indicated by black square symbols are redrawn from the data in Ref. [18].

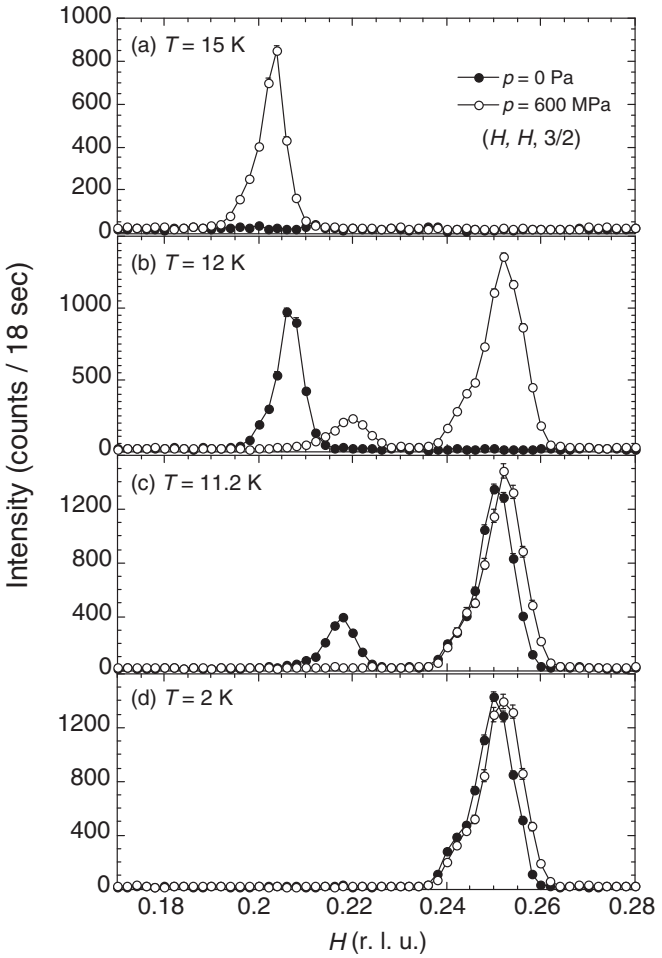

FIG. 3. Typical neutron-diffraction profiles at (a) 15, (b) 12, (c) 11.2, and (d) 2 K on cooling. The filled and open symbols denote the data measured under ambient pressure and applied p of 600 MPa, respectively.

original $T_{N1} \simeq 14$ K. The p dependence of T_{N1} is summarized in an inset of Fig. 2(a), which is a linear extension of the previous result [18]. We also found that the application of $p = 600$ MPa results in an upward shift of T_{N2} by $\sim$1 K, whereas the upward shift of T_{N2} is only $\sim$0.2 K up to 80 MPa [18].

Figures 3(a)–3(d) show typical neutron-diffraction profiles on cooling under ambient pressure and applied p of 600 MPa. At 19.4 K, which is consistent with T_{N1} ($p = 600$ MPa) obtained by the magnetic susceptibility, magnetic reflection is observed at $(q,q,3/2)$, where $q \sim 0.196$ under applied p of 600 MPa. With a decrease in T, the peak position shifts toward a higher q value, as shown in Fig. 3(a). These features correspond to the T dependence of the magnetic diffraction profiles in the PD phase under ambient pressure. At around 12 K under applied p of 600 MPa, magnetic reflection at (1/4,1/4,3/2) corresponding to the 4SL magnetic order coexists with the PD magnetic reflection, while it coexists at 11.2 K at ambient pressure, as shown in Figs. 3(b) and 3(c). Finally, below 11.8 K, the 4SL phase is realized under applied p of 600 MPa, as shown in Fig. 3(d). The T dependence of q and the integrated intensity under selected applied p are summarized in Figs. 2(b) and 2(c). We did not observe any other magnetic reflections corresponding to an emergence of other magnetic ordering, even under applied p of 600 MPa.

Here, we emphasize that the value of $q_0 \sim 0.196$, which is a magnetic modulation wave number at T_{N1}, is almost unchanged even by applied p of 600 MPa, as shown in Fig. 2(b), despite the drastic rise of T_{N1}. Taking into account that q_0 should reflect the ratio of the exchange constants, the p-independent q_0 would provide a strict condition for the p variation of the exchange constants due to the exchange striction effect. We will discuss this point later.

In order to investigate the lattice constants of CFO under $p = 600$ MPa, we also performed synchrotron radiation x-ray diffraction measurements similar to the previous study [19]. Figure 4(a) shows the temperature variations of b_m obtained by

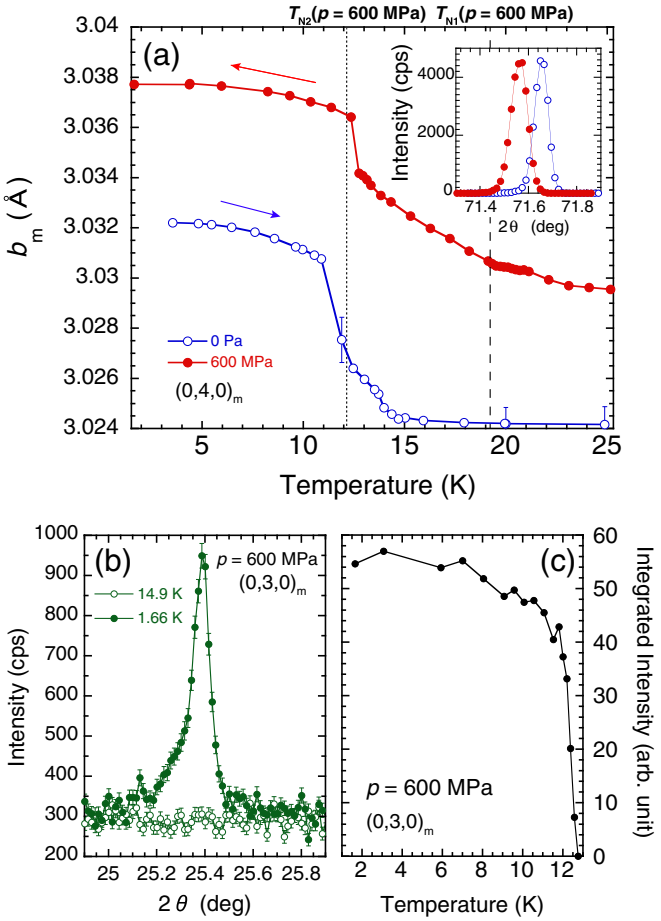

FIG. 4. (a) Temperature dependence of b_m under $p = 0$ and 600 MPa. Error bars of the $p = 600$ MPa data are within the size of the symbols. The inset shows typical x-ray profiles at 25 K under applied p of 600 MPa and at ambient pressure, which were measured with an attenuator. The $p = 0$ data are redrawn from Ref. [19], where the data are slightly shifted to absorb a tiny difference in the offset scattering angle. Note that we show the T dependence of b_m under $p = 600$ MPa during the cooling process, while that at ambient pressure in the previous study was obtained during the warming process [19]. We have observed, however, that there is no thermal hysteresis. (b) Typical x-ray profiles of the $(0,3,0)_m$ superlattice reflection under $p = 600$ MPa at 14.9 and 1.66 K. (c) Integrated intensity of the $(0,3,0)_m$ superlattice reflection under $p = 600$ MPa as a function of temperature.

$(0,4,0)_m$ reflections under $p = 0$ and 600 MPa. At T_{N1} ($p = 600$ MPa), which is determined by the magnetic susceptibility and neutron-diffraction experiments, the structural transition is smeared by the application of p, as was reported by Nakajima *et al.* [19]. With further decreasing T under applied $p = 600$ MPa, in contrast, b_m shows a discontinuous jump near T_{N2} ($p = 600$ MPa).

Figure 4(a) also shows that b_m under applied $p = 600$ MPa already elongates from the equilateral b_m even at 25 K, at which the system is in the PM phase. With decreasing T, the elongation of b_m, $\Delta b_m(p, T) \equiv b_m(p, T) - b_m(0\text{ Pa}, 25\text{ K})$, increases. At around 15 K, where the system is even in the PD phase, $\Delta b_m(600\text{ MPa}, \sim 15\text{ K})$ is comparable with $\Delta b_m(0\text{ Pa}, 4\text{ K})$ in the 4SL phase. After that, $\Delta b_m(600\text{ MPa}, T)$ continues to increase until the magnetic phase transition into the 4SL phase at T_{N2} ($p = 600$ MPa), indicating that the isosceles triangular lattice in the PD phase below 15 K under applied $p = 600$ MPa distorts more than that in the 4 SL phase at ambient pressure. On the other hand, the $(0,3,0)_m$ superlattice reflection under $p = 600$ MPa, which arise from the correspondence to the scalene triangle distortion, emerges at 12.8 K close to T_{N2} ($p = 600$ MPa), as shown in Figs. 4(b) and 4(c). These results indicate that as long as the system keeps the isosceles triangular-lattice symmetry, the magnetic phase transition into the 4SL phase does not occur. Therefore, the scalene triangle distortion is a key factor for the emergence of the 4SL magnetic ordering, as has been pointed out by several researchers [9,10].

IV. DISCUSSION

Here, we consider a uniaxial pressure effect for the spin-lattice coupled phase transition in CFO. When p is applied, a displacement of magnetic ions should modify a spin Hamiltonian due to the exchange striction effect [24,31,32]:

$$\mathcal{H} = \mathcal{H}_{\text{modified exchange}} + \mathcal{H}_{\text{lattice}}(\{\boldsymbol{u}_i\})$$
$$= J \sum_{<ij>} (1 - \alpha u_{ij}) \boldsymbol{S}_i \cdot \boldsymbol{S}_j + \mathcal{H}_{\text{lattice}}(\{\boldsymbol{u}_i\}), \qquad (1)$$

where $\boldsymbol{u}_i$ is the displacement of site i, $u_{ij} = (\boldsymbol{u}_i - \boldsymbol{u}_j) \cdot \hat{\boldsymbol{e}}_{ij}$ is the relative change in length of the bond ij ($\hat{\boldsymbol{e}}_{ij}$ is the unit vector from site i to j), and $\alpha = J^{-1} \partial J / \partial r$ is a constant. In the spin-lattice coupled system, integrating $\mathcal{H}_{\text{modified exchange}} + \mathcal{H}_{\text{lattice}}$ with $\boldsymbol{u}_i$ or u_{ij} generates an effective spin Hamiltonian including a spin-lattice coupled term [24,31,32]. In the case of the ordinary magnets (not having the spin-lattice coupling), in contrast, $\mathcal{H}_{\text{lattice}}$ can be neglected even when the exchange striction is affected by an external field at phase transition, and thus magnetic properties in the system (the phase-transition temperature, the magnetic field, or the temperature dependence of magnetic modulation wave number, and so on) can be explained only by the change in the exchange constants. For such an example, Kobayashi *et al.* quite recently reported that in a geometrically frustrated magnet $CoNb_2O_6$, q_0 in $CoNb_2O_6$ is easily modified by applied p [33]. Moreover, the p variation of the exchange constants estimated by p variation of q_0 is consistent with those estimated by the p variation of phase transition fields, and thus these results are well explained by analysis using the mean-field approximation and only $\mathcal{H}_{\text{modified exchange}}$ in $CoNb_2O_6$ [34].

In contrast, the discussion using only $\mathcal{H}_{\text{modified exchange}}$ would be unsuitable for the case of CFO. Below, we show that the enhancement of T_{N1} is not explained by the exchange striction effect with only $\mathcal{H}_{\text{modified exchange}}$. From our experiments, the temperature enhancement factor α_{obs} is

$$\alpha_{\text{obs}} \equiv \frac{T_{N1}(p = 600\text{ MPa}) = 19\text{ K}}{T_{N1}(p = 0\text{ Pa}) = 14\text{ K}} \simeq 1.36. \qquad (2)$$

Within the mean-field approximation, the magnetic phase-transition temperature T_{N1} is written as $3k_B T_{N1} = S(S+1)|J_{\max}(\boldsymbol{Q}_0)|$ in general, where k_B is the Boltzmann constant, $S = 5/2$ for CFO, $\boldsymbol{Q} = H\boldsymbol{a}^* + K\boldsymbol{b}^* + L\boldsymbol{c}^*$ is the magnetic modulation vector, $|J_{\max}(\boldsymbol{Q}_0)|$ is a Fourier-transformed maxi-

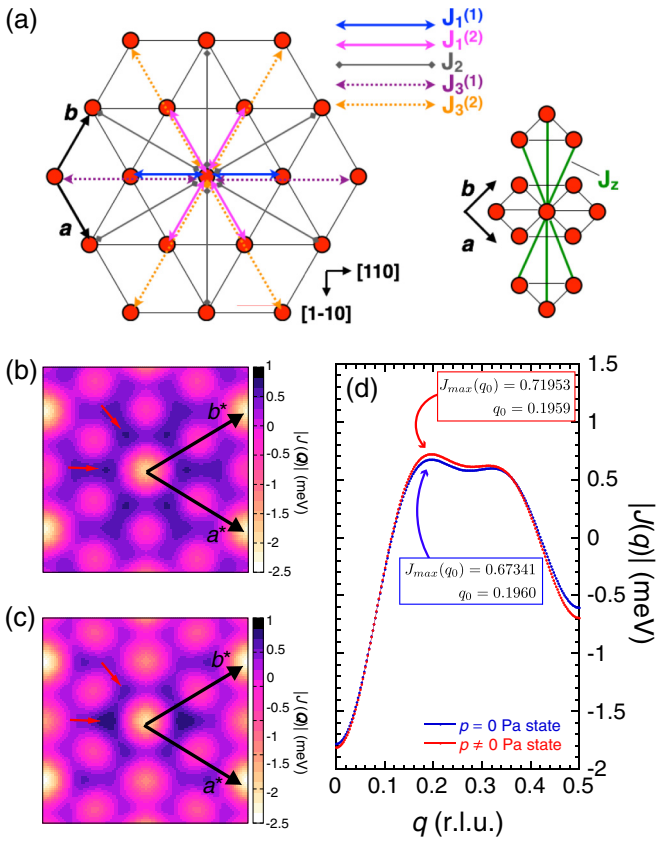

FIG. 5. (a) Paths of exchange interactions. (b),(c) $|J(\boldsymbol{Q})|$ contour map ($L = 3/2$) for (b) the $p = 0$ Pa state and (c) the (110) domain stabilized state by applied $p \parallel [1\bar{1}0]$, which is constructed using exaggerated parameter sets for visibility. (d) q dependence of $|J(q)|$. The $p = 0$ Pa state curve is constructed from the parameter sets $J_1^{(1)} = J_1^{(2)} = -0.147$, $J_2 = -0.05$, $J_3^{(1)} = J_3^{(2)} = -0.15$, $J_z = -0.05$, and the $p \neq 0$ Pa state curve is constructed from the parameter sets $J_1^{(1)} = -0.140$, $J_1^{(2)} = -0.154$, $J_2 = -0.05$, $J_3^{(1)} = -0.159$, $J_3^{(2)} = -0.155$, $J_z = -0.05$.

mum value of exchange constants, and $\boldsymbol{Q}_0$ is $\boldsymbol{Q}$ providing the maximum value of $|J(\boldsymbol{Q})|$. Therefore,

$$\alpha_{\text{calc}} \equiv \frac{\left|J_{\text{max}}^{p=600\,\text{MPa}}(\boldsymbol{Q}_0)\right|}{\left|J_{\text{max}}^{p=0\,\text{Pa}}(\boldsymbol{Q}_0)\right|} \tag{3}$$

should coincide with the temperature enhancement factor, as far as the exchange striction with only $\mathcal{H}_{\text{modified exchange}}$ is concerned.

We define the exchange constants in CFO as those shown in Fig. 5(a) [35] for a (110) domain stabilization by the application of $p \parallel [1\bar{1}0]$, as described below in detail. Taking the spin-wave analysis by Nakajima *et al.* into consideration [25,36], we have chosen the exchange constant values in meV units as $J_1^{(1)} = J_1^{(2)} = -0.147$, $J_2 = -0.05$, $J_3^{(1)} = J_3^{(2)} = -0.15$, and $J_z = -0.05$ for the $p = 0$ Pa state. As expected from the definition of the exchange constants, their Fourier transformation $J(\boldsymbol{Q})$ with these parameter values shows a sixfold symmetry along the c axis, as shown in Fig. 5(b).

Owing to the trigonal symmetry along the c axis, CFO has two other magnetic modulation vectors of $(-2q,q,3/2)$ and $(q,-2q,3/2)$, which are equivalent to $(q,q,3/2)$. As a result, three magnetic domains exist. When we apply p to the sample along the $[1\bar{1}0]$ direction, however, only the domain with $(q,q,3/2)$ magnetic modulation vector, called the (110) domain, is stabilized [37,38]. Therefore, we assume the single (110) domain state for the calculation of $|J_{\text{max}}(\boldsymbol{Q}_0)|$, hereafter. When the (110) domain is stabilized, the peaks on the (110) axis grow and the other peaks shrink, as shown in Fig. 5(c) (see red arrows). Taking into account the experimental result that the magnetic diffraction peak in the (110) domain is on the $(H,H,3/2)$ line, we can write $J[\boldsymbol{Q} = (q,q,3/2)]$ as $J(q)$:

$$\begin{aligned} J(q) = &-4J_1^{(1)}\cos(2\pi q) - 2J_1^{(2)}\cos(4\pi q) \\ &- 2J_3^{(1)}\cos(4\pi q) - 2J_3^{(2)}\cos(8\pi q) \\ &- 2J_2[\cos(6\pi q) + 1] + 2J_z[2\cos(2\pi q) + 1]. \end{aligned} \tag{4}$$

Then, we obtain $|J_{\text{max}}(\boldsymbol{Q}_0)| = |J_{\text{max}}(q_0)|$, and q_0 is just the measurement value in our experiments. The parameter sets for the $p = 0$ Pa state described above provide the $J(q)$ curve shown in Fig. 5(d) and consistently reproduce the experimental value $q_0 = 0.1960$ [39]. $|J_{\text{max}}^{p=0\,\text{Pa}}(q_0)|$ is 0.673408.

Next, on the assumption that $p = 600$ MPa is applied along the $[1\bar{1}0]$ direction, we prepared parameter sets by independently varying the values of $J_1^{(1)}$, $J_1^{(2)}$, $J_3^{(1)}$, and $J_3^{(2)}$ within $\pm 5\%$, which are considered to be the most influential parameters for $J(q)$ and q_0. Using these parameter sets, we calculated $J(q)$, q_0, and $|J_{\text{max}}^{p\neq 0\,\text{Pa}}(q_0)|$. Then, we surveyed parameter sets with consistency in the experimental result $0.1958 \leqslant q_0 \leqslant 0.1962$. In addition, we eliminated the parameter sets destabilizing the (110) domain. For simplicity, J_2 and J_z were fixed because they are smaller than J_1 and J_3.

We show one of the calculation results in Fig. 5(d). This $J(q)$ curve is obtained by using the parameter set providing the largest $|J_{\text{max}}^{p\neq 0\,\text{Pa}}(q_0)| = 0.71953$ (the values of the parameters are shown in the caption of Fig. 5). As mentioned above, q_0 is determined by the ratio of the exchange constants. We can consider that a ratio of $J_3^{(2)}$ to $J_1^{(2)}$ is the most dominant for $J(q)$ because they are interactions in the [110] direction. Thus, we can assume by intuition that if this interaction ratio is not changed under applied p, q_0 is also constant for applied p. Our calculation includes the parameter sets matching such a naive scenario. However, α_{calc} is limited to 1.07 and does not explain α_{obs} as long as the variation of J_1 and J_3 is restricted to $\pm 5\%$. This means that the exchange striction effect using $\mathcal{H}_{\text{modified exchange}}$ explains, at the most, only about 20% of α_{obs}.

Here, let us consider how large the $\pm 5\%$ variation of J_1 and J_3 is that is used in our calculation, taking into account the observed lattice deformation of CFO. From our experimental results, the b_{m} ($p = 600$ MPa, $T = 25$ K) axis elongates by 0.2%, compared to the b_{m} (0 Pa,25 K) axis. On the assumption that the ratios between the lattice parameters (a_{m}, b_{m}, and c) at ambient pressure at 2 K [10] are similar to these ratios under applied p of 600 MPa at 25 K, we estimated that the a_{m} (600 MPa,25 K) axis and the c (600 MPa,25 K) axis contract by 0.13% and 0.06%, respectively, compared to the values at ambient pressure. Using these values, we roughly estimated a change in the Fe-O-Fe bond angles, which is one of the key factors in determining the exchange constants, and found it to be 0.05%. Therefore, we conclude that the

$\pm 5\%$ variation of J_1 and J_3 is relatively large, although there is no known reason for this under the electronic bonding orbital theory. Nevertheless, α_{calc} is limited to 20% at the most within the mean-field approximation and the exchange striction effect using only $\mathcal{H}_{\mathrm{modified\ exchange}}$. Thus, we need to take $\mathcal{H}_{\mathrm{lattice}}$ into consideration to explain our experimental results.

Several specific expressions of $\mathcal{H}_{\mathrm{lattice}}$ have been proposed and the biquadratic term generated by integration of $\mathcal{H}_{\mathrm{modified\ exchange}} + \mathcal{H}_{\mathrm{lattice}}$ plays an important role in the realization of spin-lattice coupled exotic state [24,31,32]. As for CFO, this biquadratic term reasonably explains the existence of the collinear 4SL phase as the ground state. In addition to the collinear magnetic structure of the ground state in CFO, several researchers have pointed out the importance of the spin-lattice couplings for the phase transition, even at T_{N1}. For example, Quirion *et al.* suggested that the transition at T_{N1} is primary pseudoproper ferroelastic, with the spin acting as a secondary order parameter, from the ultrasonic velocity measurements and the analysis using Landau free energy [11]. Klobes *et al.* also suggested that the magnetoelastic coupling persists in the PM phase as well, using nuclear resonance scattering [20]. Keeping these studies in mind, the magnetic properties of CFO such as $T_{\mathrm{N1,2}}$, q_0, or T dependence of q should also be treated by a theory including the appropriate spin-lattice coupling, in addition to the magnetic structures.

Finally, we show the temperature dependence of the dielectric constant under applied p in Fig. 2(d). We found that the temperature dependence of the dielectric constant is drastically changed with large thermal hysteresis by applied p of 600 MPa. However, we did not observe the ferroelectric polarization and the T dependence of an imaginary part of the dielectric constant remains 0 even under applied p of 600 MPa. Recently, Terada *et al.* reported that spiral magnetic ordering with ferroelectricity is induced by isotropic pressure $\sim$3 GPa [17]. Taking into account this report, one possible explanation for this anomalous dielectric property is that the drastic change in T dependence of ϵ may reflect the precursor of the emergence of spiral magnetic ordering with ferroelectricity. The application of a larger magnitude of p may be a promising way to investigate the spin-lattice coupled multiferroic phase.

V. CONCLUSIONS

We performed magnetic susceptibility, dielectric constant, neutron-diffraction, and synchrotron radiation x-ray diffraction measurements on a spin-lattice coupled system $CuFeO_2$ under applied uniaxial pressure p up to 600 MPa. We found that the value of q_0 is not changed even by applied p of 600 MPa despite a drastic rise of T_{N1} by as much as 5 K, and that the applied p of 600 MPa causes remarkable change in the b_{m} lattice constant beyond the spontaneous lattice distortion. Our calculation of the observed enhancement of T_{N1} within the mean-field approximation and the exchange striction effect suggests that the lattice degree of freedom via the spin-lattice coupling should be indispensable for the determination of the magnetic properties besides the magnetic structures in $CuFeO_2$.

Moreover, we found that the temperature dependence of the dielectric constant is drastically changed with large thermal hysteresis by applied p of 600 MPa. To elucidate whether this dielectric anomaly stems from the spin-lattice coupled magnetoelectric effect, further study of the dielectric anomaly would be needed.

ACKNOWLEDGMENTS

We thank the Helmholtz-Zentrum Berlin (HZB) for the allocation of neutron beam time. The neutron-diffraction experiments at HZB were carried out in accordance with Proposal No. PHY-01-3177, which was transferred from HQR(T1-1) installed at JRR-3 with the approval of the Institute for Solid State Physics, The University of Tokyo (Proposal No. 12658), Japan Atomic Energy Agency, Tokai, Japan. This study was approved by the Photon Factory Program Advisory Committee (Proposal No. 2013G676). This work was supported by a Grant-in-Aid for Scientific Research (C) (Grants No. 23540424 and No. 26400369) from the Japan Society for the Promotion of Science.

[1] R. Moessner and A. P. Ramirez, Phys. Today **59**(2), 24 (2006).
[2] F. Becca and F. Mila, Phys. Rev. Lett. **89**, 037204 (2002).
[3] K. Kodama, M. Takigawa, M. Horvatic, C. Berthier, H. Kageyama, Y. Ueda, S. Miyahara, F. Becca, and F. Mila, Science **298**, 395 (2002).
[4] Y. Yamashita and K. Ueda, Phys. Rev. Lett. **85**, 4960 (2000).
[5] O. Tchernyshyov, R. Moessner, and S. L. Sondhi, Phys. Rev. Lett. **88**, 067203 (2002).
[6] Y. Tokura, S. Seki, and N. Nagaosa, Rep. Prog. Phys. **77**, 076501 (2014).
[7] T. Kimura, J. C. Lashley, and A. P. Ramirez, Phys. Rev. B **73**, 220401(R) (2006).
[8] T. Nakajima, S. Mitsuda, S. Kanetsuki, K. Tanaka, K. Fujii, N. Terada, M. Soda, M. Matsuura, and K. Hirota, Phys. Rev. B **77**, 052401 (2008).
[9] F. Ye, Y. Ren, Q. Huang, J. A. Fernandez-Baca, P. Dai, J. W. Lynn, and T. Kimura, Phys. Rev. B **73**, 220404(R) (2006).
[10] N. Terada, S. Mitsuda, H. Ohsumi, and K. Tajima, J. Phys. Soc. Jpn. **75**, 023602 (2006).
[11] G. Quirion, M. J. Tagore, M. L. Plumer, and O. A. Petrenko, Phys. Rev. B **77**, 094111 (2008).
[12] G. Quirion, M. L. Plumer, O. A. Petrenko, G. Balakrishnan, and C. Proust, Phys. Rev. B **80**, 064420 (2009).
[13] M. L. Plumer, Phys. Rev. B **78**, 094402 (2008).
[14] T. T. A. Lummen, C. Strohm, H. Rakoto, and P. H. M. van Loosdrecht, Phys. Rev. B **81**, 224420 (2010).
[15] N. Terada, S. Mitsuda, Y. Tanaka, Y. Tabata, K. Katsumata, and A. Kikkawa, J. Phys. Soc. Jpn. **77**, 054701 (2008).
[16] N. Terada, T. Osakabe, and H. Kitazawa, Phys. Rev. B **83**, 020403 (2011).

[17] N. Terada, D. D. Khalyavin, P. Manuel, T. Osakabe, P. G. Radaelli, and H. Kitazawa, Phys. Rev. B **89**, 220403 (2014).

[18] T. Nakajima, S. Mitsuda, K. Takahashi, K. Yoshitomi, K. Masuda, C. Kaneko, Y. Honma, S. Kobayashi, H. Kitazawa, M. Kosaka, N. Aso, Y. Uwatoko, N. Terada, S. Wakimoto, M. Takeda, and K. Kakurai, J. Phys. Soc. Jpn. **81**, 094710 (2012).

[19] T. Nakajima, Y. Iguchi, H. Tamatsukuri, S. Mitsuda, Y. Yamasaki, H. Nakao, and N. Terada, J. Phys. Soc. Jpn. **82**, 114711 (2013).

[20] B. Klobes, M. Herlitschke, K. Z. Rushchanskii, H.-C. Wille, T. T. A. Lummen, P. H. M. van Loosdrecht, A. A. Nugroho, and R. P. Hermann, Phys. Rev. B **92**, 014304 (2015).

[21] S. Mitsuda, N. Kasahara, T. Uno, and M. Mase, J. Phys. Soc. Jpn. **67**, 4026 (1998).

[22] In Ref. [20], Klobes *et al.* have suggested that the magnetic structure in the range $T_{N2} \leqslant T \leqslant T_{N1}$ is incompatible with the sinusoidal one. This suggestion, however, does not conflict with our results and discussion because our discussion is independent of specific magnetic structures.

[23] M. Mekata, N. Yaguchi, T. Takagi, T. Sugino, S. Mitsuda, H. Yoshizawa, N. Hosoito, and T. Shinjo, J. Phys. Soc. Jpn. **62**, 4474 (1993).

[24] F. Wang and A. Vishwanath, Phys. Rev. Lett. **100**, 077201 (2008).

[25] T. Nakajima, A. Suno, S. Mitsuda, N. Terada, S. Kimura, K. Kaneko, and H. Yamauchi, Phys. Rev. B **84**, 184401 (2011).

[26] S. Kimura, T. Fujita, N. Nishihagi, H. Yamaguchi, T. Kashiwagi, M. Hagiwara, N. Terada, Y. Sawai, and K. Kindo, Phys. Rev. B **84**, 104449 (2011).

[27] In Ref. [17], q_0 is described in monoclinic notation. Then, q_0 is varied from ∼0.39 (0 Pa) to ∼0.37 (5 GPa) by the isotropic pressure.

[28] T. R. Zhao, M. Hasegawa, and H. Takei, J. Cryst. Growth **166**, 408 (1996).

[29] T. Nakajima, S. Mitsuda, T. Nakamura, H. Ishii, T. Haku, Y. Honma, M. Kosaka, N. Aso, and Y. Uwatoko, Phys. Rev. B **83**, 220101 (2011).

[30] The value of $T_{N1} \sim 15.3$ K is relatively high (usually $T_{N1} \simeq 14$ K in some reports [9]). This may be accidentally caused by effective application of p for the sample because of experimental setup conditions.

[31] K. Penc, N. Shannon, and H. Shiba, Phys. Rev. Lett. **93**, 197203 (2004).

[32] D. L. Bergman, R. Shindou, G. A. Fiete, and L. Balents, Phys. Rev. B **74**, 134409 (2006).

[33] S. Kobayashi, S. Hosaka, H. Tamatsukuri, T. Nakajima, S. Mitsuda, K. Prokeš, and K. Kiefer, Phys. Rev. B **90**, 060412 (2014).

[34] S. Mitsuda (unpublished).

[35] Note that the definition for $J_1^{(1)}$ and $J_1^{(2)}$ is different from the one used in Refs. [25,36,40]. In the spin-wave analysis in these papers, Nakajima *et al.* defined $J_1^{(1)}$ and $J_1^{(2)}$ based on the magnetostriction effect including the displacement of O^{2-} ions. On the other hand, we discuss the magnetic phase transition at T_{N1}, and thus we consider only the exchange striction effect based on the relative change in the lattice distance, instead of the magnetostriction effect depending on the magnetic structure.

[36] T. Nakajima, N. Terada, S. Mitsuda, and R. Bewley, Phys. Rev. B **88**, 134414 (2013).

[37] S. Mitsuda, K. Yoshitomi, T. Nakajima, C. Kaneko, H. Yamazaki, M. Kosaka, N. Aso, Y. Uwatoko, Y. Noda, M. Matsuura, N. Terada, S. Wakimoto, M. Takeda, and K. Kakurai, J. Phys.: Conf. Ser. **340**, 012062 (2012).

[38] T. Nakajima, S. Mitsuda, T. Haku, K. Shibata, K. Yoshitomi, Y. Noda, N. Aso, Y. Uwatoko, and N. Terada, J. Phys. Soc. Jpn. **80**, 014714 (2011).

[39] Although the values of these parameters reproduce the q_0 value, they are slightly different from those in Refs. [25,36,40]. Taking into account that the exchange parameters at the low temperature should differ from those at T_{N1}, we believe that this slight difference is appropriate.

[40] T. Nakajima, S. Mitsuda, J. T. Haraldsen, R. S. Fishman, T. Hong, N. Terada, and Y. Uwatoko, Phys. Rev. B **85**, 144405 (2012).